^{131}I therapy mediated by sodium/iodide symporter combined with kringle 5 has a synergistic therapeutic effect on glioma

SHUO SHI, MIN ZHANG, RUI GUO, MIAO ZHANG, JIAJIA HU, YUN XI, YING MIAO and BIAO LI

Department of Nuclear Medicine, Ruijin Hospital, Shanghai Jiaotong University School of Medicine, Shanghai 200025, P.R. China

Received July 1, 2015; Accepted August 14, 2015

DOI: 10.3892/or.2015.4420

Abstract. Glioblastoma (GBM) is the most common and most aggressive primary brain tumor; the prognosis of patients with GBM remains poor. The sodium/iodide symporter (NIS) can be used to absorb several isotopes, such as ^{131}I for nuclear medicine imaging and radionuclide therapy. Previously, we found that the early growth response-1 (Egr1) promoter had an ^{131}I radiation positive feedback effect on the *NIS* gene. Kringle 5 (K5), a kringle domain of plasminogen, induced endothelial cell apoptosis. We investigated the effect of K5 combined with the ^{131}I radiation positive feedback effect (Egr1-NIS) for treating malignant U87 glioma cells using a lentiviral vector. We successfully constructed a stable U87 glioma cell line, U87-K5-Egr1-NIS. The radio-inducible Egr1 promoter induced an ^{131}I radiation positive feedback effect absorbed by NIS. Mediated by ^{131}I, K5 increased glioma cell apoptosis; ^{131}I radiation also increased endothelial cell sensitivity to K5-induced apoptosis. The combined therapy had a synergistic effect on the antitumor efficacy of glioma treatment, not only increasing tumor cell apoptosis but also significantly inhibiting tumor cell proliferation and reducing capillary density in U87 glioma tissues.

Introduction

Glioblastoma (GBM) is the most common and most aggressive primary brain tumor. Despite aggressive surgery, radiotherapy and chemotherapy, the prognosis of GBM remains poor. Gene therapy is increasingly being explored as a novel therapeutic option.

The sodium/iodide symporter (NIS), which facilitates iodide uptake driven by sodium ion gradients across the plasma membrane, is a simple and useful reporter. Iodine radioisotopes were first used as thyroid function tracers and subsequently for treating hyperthyroidism and benign thyroid diseases (1). NIS can absorb several isotopes, such as ^{99m}Tc, ^{188}Re and ^{131}I, which are important for nuclear medicine imaging and radionuclide therapy (2-4). Therefore, as a therapeutic ectopic gene, *NIS* has been used in numerous preclinical studies on the treatment of a variety of cancers (5-7). Vadysirisack *et al* showed that the radioiodine uptake is proportionate to the total NIS protein level and that enhancing NIS protein expression improves reporter sensitivity and the therapeutic efficacy of radioiodine therapy (8). The early growth response-1 (Egr1) promoter is a radio-inducible promoter that can be promoted by ionizing radiation (9) and induce the expression of downstream target genes. Our laboratory detected an ^{131}I radiation positive feedback effect in a Bac-Egr1-hNIS (a baculovirus-containing Egr1-promoted NIS) system in U87 glioma cells (10).

Various studies have suggested that antiangiogenic drugs enhance the tumor response to radiotherapy (11) or radionuclide therapy (5,12). Kringle 5 (K5), a kringle domain of plasminogen, can induce apoptosis in dermal microvessel endothelial cells (ECs) (13,14) and inhibit the proliferation of basic fibroblast growth factor-stimulated calf pulmonary arterial EC and bovine adrenal capillary ECs (14,15). In the present study, we constructed a stable U87 cell line expressing K5 and investigated the effect of K5 combined with the ^{131}I radiation positive feedback effect (Egr1-NIS) for treating malignant U87 glioma.

Materials and methods

Cell lines and animals. The U87 human glioma cell line [American Type Culture Collection (ATCC), Manassas, VA, USA] and HUVECs and the 293T cell line (Cell Bank of the Chinese Academy of Science, Shanghai, China) were maintained in Dulbecco's modified Eagle's medium (DMEM) supplemented with 10% fetal bovine serum, 100 U/ml penicillin and 100 mg/ml streptomycin in 5% CO_2 at 37˚C. Twenty-four male BALB/c nude mice (4-weeks old) were purchased from Shanghai Slaccas Experiment Animal Corporation (Shanghai Institute for Biological Science, Shanghai, China).

Plasmid construction and lentiviral preparation. The pcDNA3.1-hNIS vector was kindly provided by Dr Sissy Jhiang (Ohio University, Athens, OH, USA). The pGL3-Egr1-Luc plasmid, containing the luciferase gene under the control of the Egr1 promoter, was a kind gift from Gerald Thiel

Correspondence to: Dr Biao Li, Department of Nuclear Medicine, Ruijin Hospital, Shanghai Jiaotong University School of Medicine, 197 Ruijin Er Road, Shanghai 200025, P.R. China
E-mail: lb10363@rjh.com.cn

Key words: early growth response-1 promoter, gene therapy, glioma, kringle 5, sodium/iodide symporter

(University of Saarland Medical Center, Homburg, Germany). The pET22b-K5 plasmid (His-tagged) was previously constructed in our laboratory (5). The pLVX-CMV-Puro (puromycin) expression vector was purchased from Clontech (Takara, Dalian, China). The *NIS*, *EGR1* and *K5* (His-tagged) genes were PCR-amplified separately from pcDNA3.1-hNIS, pGL3-Egr1-Luc and pET22b-K5, respectively, and then cloned into the pLVX-CMV-Puro vector to construct pLVX-CMV-K5-Egr1-NIS, pLVX-CMV-K5-Egr1-GFP and pLVX-CMV-GFP-Egr1-NIS plasmids, respectively. The resulting plasmids were recombined with a destination vector according to the manufacturer's instructions. The viral particles were produced and amplified in 293T cells.

In vitro infection with the recombinant lentiviruses. U87 cells were infected at an multiplicity of infection (MOI) of 20 ($2x10^6$ pfu/10^5 cells in 1 ml complete media) with pLVX-CMV-K5-Egr1-NIS, pLVX-CMV-K5-Egr1-GFP and pLVX-CMV-GFP-Egr1-NIS, or not transduced. To generate cell lines harboring the K5-expressing antibiotic marker puromycin as controlled by the cytomegalovirus (CMV)-enhancer/promoter (NIS was controlled by the Egr1 promoter), cells were selected in 0.5 μg/ml puromycin (Sigma, Sydney, Australia) for the required duration. The stable cell lines U87-K5-NIS, U87-K5-GFP and U87-GFP-NIS were constructed.

Western blot analyses. U87-K5-NIS, U87-K5-GFP, U87-GFP-NIS and U87 cell lysates were prepared using standard methods. To detect NIS expression following ^{131}I irradiation, Na^{131}I (final concentration, 3.7 MBq/ml) was added into the U87-K5-NIS and U87-GFP-NIS cell cultures for 24 h, and the cell lysates were obtained for western blot analysis. To detect K5 expression in the cell supernatants, western blotting was performed according to a previous study (16). K5 and NIS proteins were separately run on 7 and 15% Tris-glycine gels, respectively. Mouse anti-NIS (Millipore, Boston, MA, USA) and mouse anti-His-tag (Abgent, Suzhou, China) antibodies were used at a 1:500 dilution at 4˚C overnight, followed by incubation with the secondary anti-mouse antibody and with peroxidase-conjugated goat anti-mouse immunoglobulin G (1:2,500; Santa Cruz Biotechnology, Santa Cruz, CA, USA) for 2 h at 4˚C. Anti-β-actin (1:5,000; Abgent) was used as the loading control. Immunodetection was carried out using an ECL Western Blot Detection kit (Thermo Scientific, Pierce, Waltman, MA, USA).

In vitro iodide uptake studies. We determined ^{125}I uptake and efflux in triplicate as previously described (17). The day before the experiment, U87-K5-NIS, U87-K5-GFP, U87-GFP-NIS and U87 cells were plated ($2x10^5$ cells/well) into 24-well plates. After 24 h, 500 μl HBSS containing 3.7 kBq ^{125}I and 10 μmol/l sodium iodide (NaI) was added. The cells were incubated at 37˚C for 5-120 min, washed twice with ice-cold HBSS and lysed using 0.5 mol/l NaOH. The radioactivity (counts/min, cpm) of the cell lysates was measured using an automatic γ-counter (Shanghai Rihuan Company, Shanghai, China).

In vitro clonogenic assay. U87-K5-NIS, U87-K5-GFP, U87-GFP-NIS and U87 cells were plated on 10-cm culture dishes ($6x10^6$ cells/dish); 4.6 MBq ^{131}I in HBSS was added to each dish. After 8 h, the cells were washed three times with HBSS, trypsinized and plated into 6-well culture plates (1,000 cells/well). On day 7, the cells were stained with 1 ml crystal violet staining solution (Beyotime Institute of Biotechnology, Shanghai, China) for 10 min, and colonies containing >50 cells were counted; the results are expressed as the percentage of surviving cells. The survival rate was expressed as the percentage of colonies to that of the blank group without ^{131}I incubation. Data are presented as the means ± SD.

Cytotoxic effect of K5 on HUVECs in vitro. HUVECs were plated into 6-well culture plates ($5x10^5$ cells/well). U87-K5-NIS, U87-K5-GFP, U87-GFP-NIS and U87 cells were plated on 10-cm culture dishes ($5x10^6$ cells/dish). After a 24-h incubation, the U87-K5-NIS, U87-K5-GFP, U87-GFP-NIS and U87 cells were washed three times with phosphate-buffered saline (PBS) and 3 ml DMEM was added to each dish. After 12 h, the medium was aspirated and centrifuged at 800 x g for 5 min. The HUVEC medium was removed, and then the centrifuged medium was added to the HUVECs. After 24 h, the HUVECs were trypsinized and plated into 6-well culture plates (500 cells/well). On day 7, the cells were stained with 1 ml crystal violet staining solution (Beyotime Institute of Biotechnology) for 10 min, and colonies containing >50 cells were counted.

Establishment of xenograft tumors in nude mice. The right flanks of the BALB/c nude mice were s.c. injected with U87-K5-NIS, U87-K5-GFP, U87-GFP-NIS or U87 cells in 100 μl PBS. The mice were euthanized by cervical vertebra dislocation at the end of the experiments. The animal studies were approved by the local Ethics Committee (Shanghai Jiao Tong University School of Medicine, Shanghai, China) and performed according to the principles of ethics related to animal experimentation.

Micro-single-photon emission computed tomography/computed tomography (SPECT/CT) imaging. To detect iodide uptake by NIS as promoted by the Egr1 promoter after iodide irradiation, three U87-K5-NIS tumor-bearing mice were i.v. injected with 18.5 MBq ^{125}I. Anesthesia was administered and maintained by isoflurane inhalation, and the mice were positioned spread prone and scanned using a small-animal micro-SPECT scanner (Bioscan, Washington, DC, USA) at 1 and 24 h after ^{125}I injection. Without moving the mice, CT images were acquired (CT dose index; CTDI = 6.1 cGy) before whole-body nanoSPECT images (10 sec/frame for systematic scans) were obtained. Two days after the first ^{125}I injection and microSPECT/CT imaging, U87-K5-NIS tumor-bearing mice were i.v. injected with 18.5 MBq ^{125}I again and microSPECT/CT imaging was performed at 1 h after the injection. The images were processed and were reconstructed using Nuclear v1.02 software; images were acquired using HiSPECT 1.4.2 software and analyzed using InVivoScope 1.44 software (all from Bioscan). Regions of interest (ROIs) were drawn around the visible organs, and the radioactivity per volume unit (Conc) in the ROIs was measured using InVivoScope 1.44.

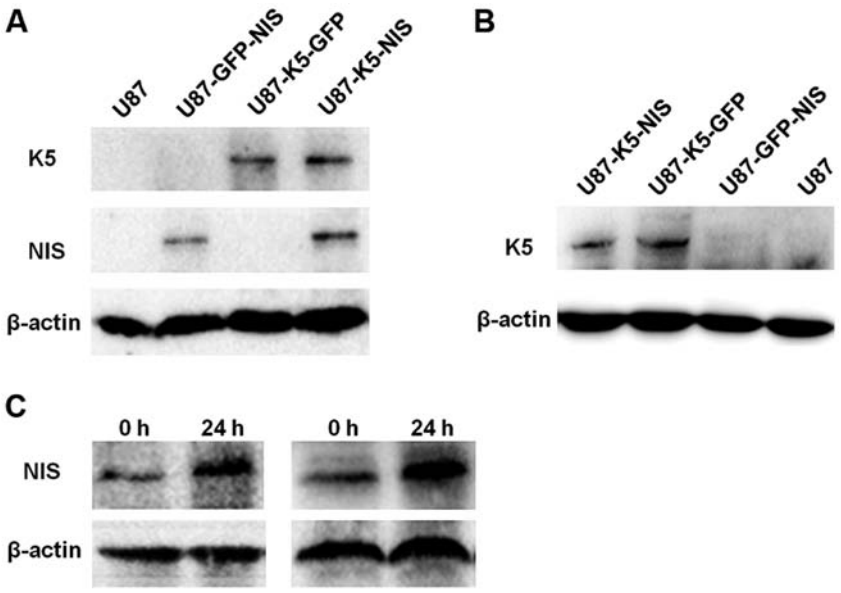

Figure 1. Western blot analysis of K5 and NIS expression. (A) K5 and NIS expression in the U87-K5-NIS, U87-K5-GFP, U87-GFP-NIS and U87 cells. (B) K5 expression in the supernatant of the different cell lines. (C) NIS expression in the U87-K5-NIS and U87-GFP-NIS cells before and after a 24-h ^{131}I irradiation.

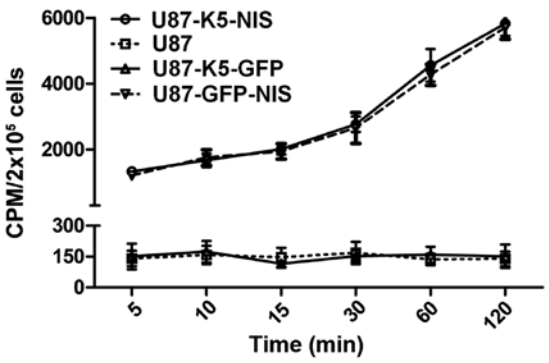

Figure 2. ^{125}I uptake assays. ^{125}I uptake by the U87-K5-NIS, U87-K5-GFP, U87-GFP-NIS and U87 cells at 5-120 min.

In vivo ^{131}I therapy. One day before ^{131}I administration, the animals received a 0.5-ml i.p. injection of 0.9% NaI solution to block the thyroid uptake of any free radioactive iodide. Treatment was initiated when the tumors had grown to 3-5 mm in diameter (~70 mm^3). U87-K5-NIS, U87-K5-GFP, U87-GFP-NIS or U87 tumor-bearing mice were i.v. injected with 37 MBq ^{131}I on day 1 and 3. Tumor size was measured on day 7 after the injection and every three days thereafter up to day 25 using calipers; tumor volume was calculated as follows: Volume (mm^3) = (L x W^2)/2 (18).

Histology and immunohistochemistry. At 25 days after ^{131}I administration, the animals were sacrificed, and the tumors were cryosectioned (5 μm) and subjected to immunofluorescence and immunohistochemical analysis using mouse anti-CD31 (1:50; Dako, Glostrup, Denmark), rabbit anti-human caspase-3 (1:30; Epitomics, Burlingame, CA, USA) and rabbit anti-human Ki-67 antibodies (1:200; Thermo Scientific, Fremont, CA, USA). Immunohistochemical analysis was performed using Image-Pro Plus software (Media Cybernetics, Rockville, MD, USA). The integral optical density (IOD) of every visual field was calculated for each section. Data are represented as means ± SD. Capillary density was defined as the number of CD31$^+$ ECs/high-power field (hpf; x200). Five hpfs were counted per section from six sections/tumor tissue in three animals/group.

Statistical analysis. Data were analyzed using GraphPad Prism software (version 5.0; GraphPad Software, Inc., La Jolla, CA, USA); the means ± SD are presented. Statistical analyses were performed using two-tailed Student's t-tests for differences between groups and ANOVA for differences among groups. For all analyses, $P<0.05$ was considered to indicate a statistically significant result.

Results

K5 and NIS expression. To investigate K5 and NIS expression in the U87-K5-NIS, U87-K5-GFP, U87-GFP-NIS and U87 cell lines, we detected K5 expression in the supernatant of these cell lines using western blotting. K5 was expressed in the U87-K5-NIS and U87-K5-GFP cells (Fig. 1A) and their supernatant (Fig. 1B), but not in the U87-GFP-NIS and U87 cells (Fig. 1A) or their supernatant (Fig. 1B). NIS was expressed in the U87-K5-NIS and U87-GFP-NIS cells but not in the U87-K5-GFP or U87 cells (Fig. 1A). Western blotting also showed weak expression of NIS protein in the U87-K5-NIS and U87-GFP-NIS cells without irradiation, but higher NIS expression after a 24-h ^{131}I irradiation (Fig. 1C).

In vivo ^{125}I uptake in cell lines. The functional activity of NIS protein was clearly shown by its cellular iodide uptake. ^{125}I uptake by the U87-K5-NIS and U87-GFP-NIS cells varied with the duration of incubation. Following its addition to the U87-K5-NIS and U87-GFP-NIS cells, ^{125}I was gradually absorbed by NIS protein and was ~6,000 cpm at 120 min; no functional iodide uptake was observed in the U87-K5-GFP and U87 cells (Fig. 2).

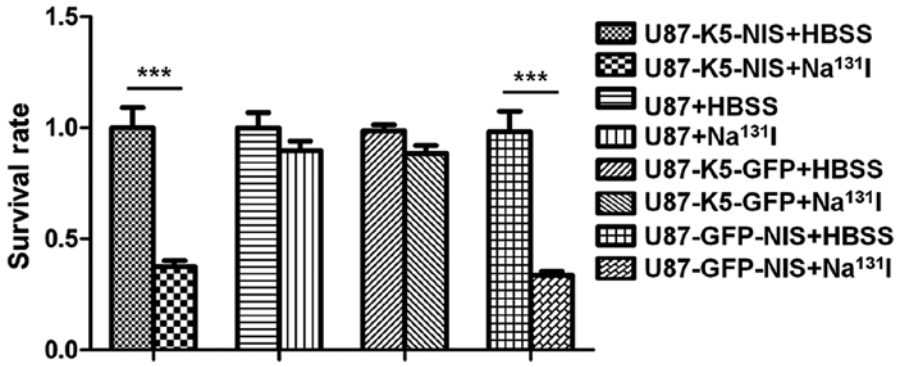

Figure 3. Cytotoxic effect of ^{131}I on cell lines *in vitro*. U87-K5-NIS, U87-K5-GFP, U87-GFP-NIS and U87 cells were incubated with ^{131}I in HBSS for 8 h. Subsequently, the cells were washed with HBSS, trypsinized and plated into 6-well culture plates. The survival rate is expressed as the percentage of colonies to that of the blank group without ^{131}I incubation. Data are the means ± SD. ***p<0.001.

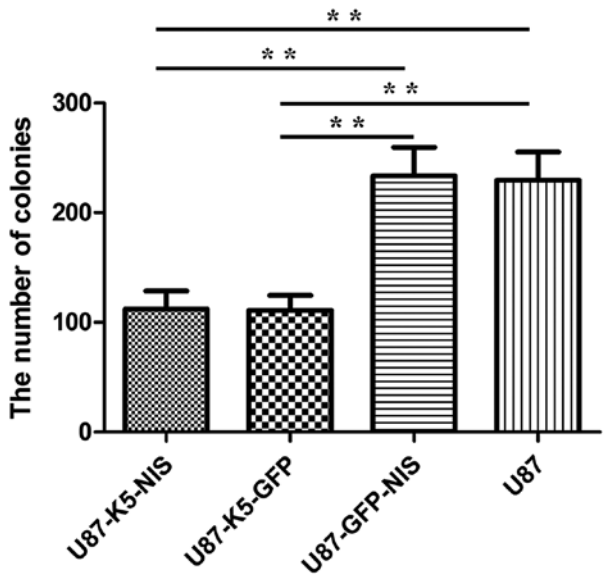

Figure 4. Cytotoxic effect of K5 on HUVECs *in vitro*. *In vitro* clonogenic assays were performed to determine the effect of the K5-containing medium of U87-K5-NIS and U87-K5-GFP cells and the K5-absent medium of U87-GFP-NIS and U87 cells on HUVECs. Data are the means ± SD. **p<0.01.

^{131}I reduces the survival of U87 cells expressing NIS in vitro. *In vitro* clonogenic assays were performed to determine the cytotoxic effect of ^{131}I on U87-K5-NIS, U87-K5-GFP, U87-GFP-NIS and U87 cells. ^{131}I had a significant cytotoxic effect on the U87-K5-NIS and U87-GFP-NIS cells when compared to the effect on the U87-K5-GFP and U87 cells (P<0.001) and the control HBSS-treated U87-K5-NIS, U87-K5-GFP, U87-GFP-NIS and U87 cells (P<0.001) (Fig. 3).

Cytotoxic effect of K5 on HUVECs in vitro. *In vitro* clonogenic assays were performed to determine the effect of K5 on HUVECs. Compared to the U87-GFP-NIS and U87 cell culture medium, the medium containing K5 secreted by the U87-K5-NIS and U87-K5-GFP cells had a significant cytotoxic effect on the HUVECs (P<0.01) (Fig. 4).

In vivo imaging of ^{125}I biodistribution in mice bearing U87-K5-NIS xenografts. Significant radioactive uptake was observed in the U87-K5-NIS tumors at 1 h after ^{125}I injection (Fig. 5A); however, ^{125}I uptake was not detectable in the U87-K5-NIS tumors 24 h after ^{125}I injection (Fig. 5B). Two days after the first ^{125}I injection, the U87-K5-NIS tumor-bearing mice were i.v. injected with 18.5 MBq ^{125}I again, and the radioactivity of the U87-K5-NIS tumors was increased significantly (Fig. 5C). The images were processed and ROIs were created by CT positioning during SPECT imaging to define the tissues described above; the obtained Conc value was 0.1240±0.0201 μCi/mm^3 at 1 h after the first ^{125}I injection, which was much higher than that at 24 h after ^{125}I injection (0.0051±0.0002 μCi/mm^3) (P<0.001). Two days later at 1 h after the ^{125}I injection, the Conc value was 0.3243±0.0333 μCi/mm^3, which was almost three times higher than that at 1 h after the first ^{125}I injection (P<0.001) (Fig. 5D). Significant radioiodine accumulation was also observed in tissues expressing endogenous *NIS*, including the thyroid and stomach, and in the urinary bladder due to renal elimination (Fig. 5A-C).

Therapeutic effects of K5 combined with ^{131}I in U87 xenograft tumors expressing K5 and NIS in vivo. We initiated ^{131}I therapy when the tumors were 3-5 mm in diameter (~70 mm^3). K5 combined with ^{131}I significantly inhibited U87-K5-NIS tumor growth as compared to the ^{131}I-treated U87-GFP-NIS, U87-K5-GFP and U87 tumors (P<0.001). There was no significant difference between U87-GFP-NIS and U87-K5-GFP tumor growth (P>0.05), but these two tumors grew slowly compared with the U87 tumors (P<0.05) (Fig. 6A). Therapy did not affect mouse food intake or physical activity. During treatment, the weight of the U87-K5-NIS tumor-bearing mice increased at almost the same rate as the U87-GFP-NIS, U87-K5-GFP and U87 tumor-bearing mice (P>0.05) (Fig. 6B).

Immunohistochemical and immunofluorescence analysis. Fig. 7 depicts representative images of the indirect tumor xenograft immunohistochemical staining. Immunohistochemical analysis revealed higher caspase-3 protein expression in the ^{131}I-treated U87-K5-NIS xenograft cells as compared with the ^{131}I-treated U87-GFP-NIS (P<0.001), U87-K5-GFP (P<0.001) and U87 (P<0.001) xenograft cells, but lower Ki-67 protein expression in the ^{131}I-treated U87-K5-NIS xenograft cells as compared with the other three groups (P<0.01) (Fig. 7A and B). There was higher caspase-3 protein expression in the

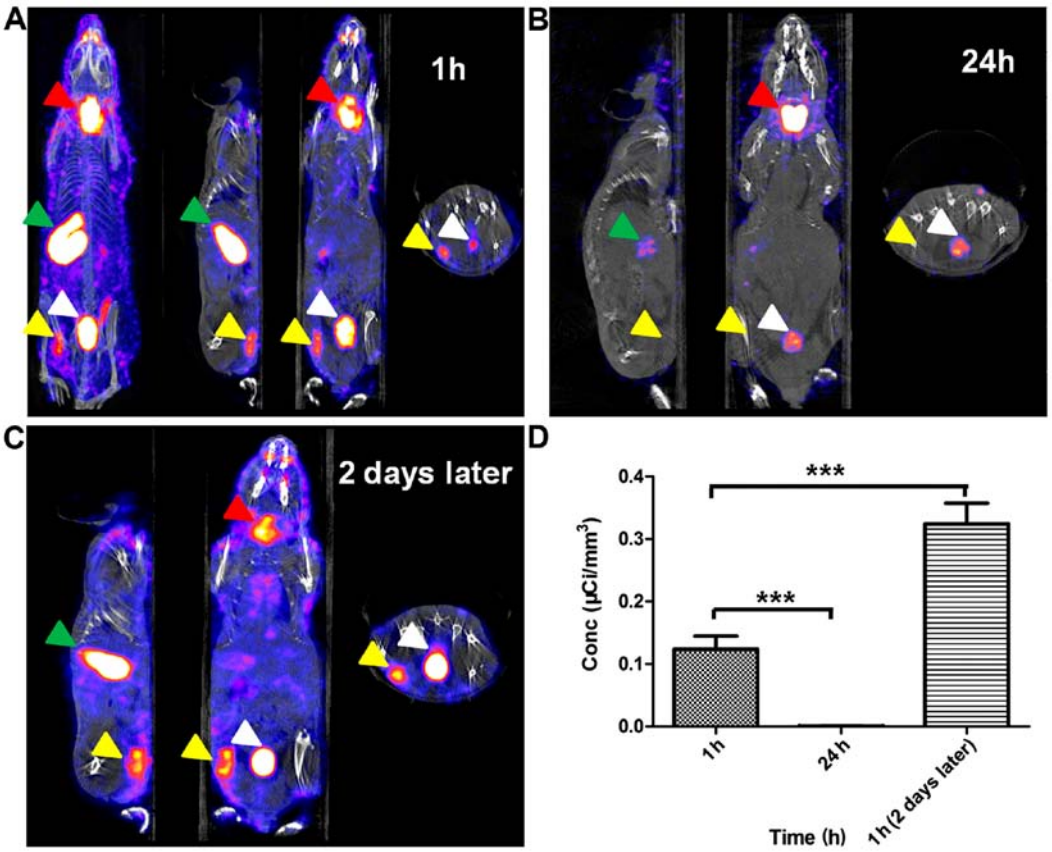

Figure 5. MicroSPECT/CT images of mice bearing U87-K5-NIS tumors in which NIS was promoted by the Egr1 promoter. (A) ^{125}I uptake 1 h after injection with 18.5 MBq ^{125}I. (B) ^{125}I uptake 24 h after injection with 18.5 MBq ^{125}I. (C) ^{125}I uptake two days after the first injection. (D) Tumor Conc values. Yellow arrowhead, U87-K5-NIS tumor; green arrowhead, stomach; red arrowhead, thyroid; white arrowhead, urinary bladder; ***p<0.001.

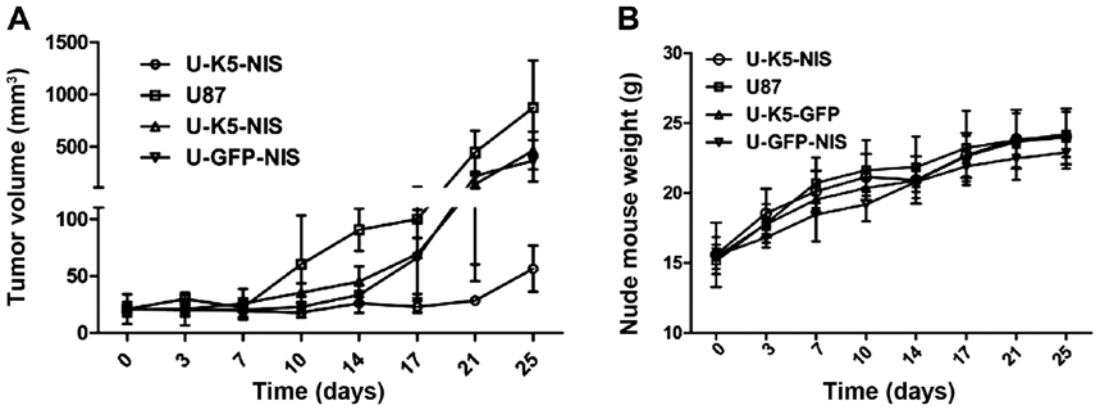

Figure 6. Therapeutic effects of K5 and ^{131}I on U87-K5-NIS xenografts. (A) U87-K5-NIS, U87-GFP-NIS and U87 xenograft growth was measured during the 25-day period following ^{131}I injection. Data are the means ± SD. (B) Weight of the mice during the 25-day period following ^{131}I injection. Data are the means ± SD.

U87-GFP-NIS and U87-K5-GFP xenograft cells compared with the U87 xenograft cells (P<0.05), but the Ki-67 protein expression levels in the U87-GFP-NIS, U87-K5-GFP and U87 xenograft cells was nearly identical (Fig. 7A and B). Immunofluorescence revealed fewer CD31$^+$ capillaries in the U87-K5-NIS group compared with the U87-GFP-NIS (P<0.01), U87-K5-GFP (P<0.01) and U87 (P<0.001) groups. There were fewer CD31$^+$ capillaries in the U87-K5-GFP group as compared with the U87-GFP-NIS (P<0.05) and U87 (P<0.05) groups (Fig. 7A and B).

Discussion

We tested the hypothesis that radioiodide (^{131}I) therapy mediated by the *NIS* gene and the antiangiogenic agent K5 would have a synergistic effect on therapeutic antitumor efficacy in glioma. To increase the accumulation and radiotherapeutic effect of ^{131}I, the radio-inducible Egr1 promoter was used as the *NIS* gene promoter, producing an ^{131}I radiation positive feedback effect. The combined therapy limited glioma growth and progression more effectively. Our results indicated that the

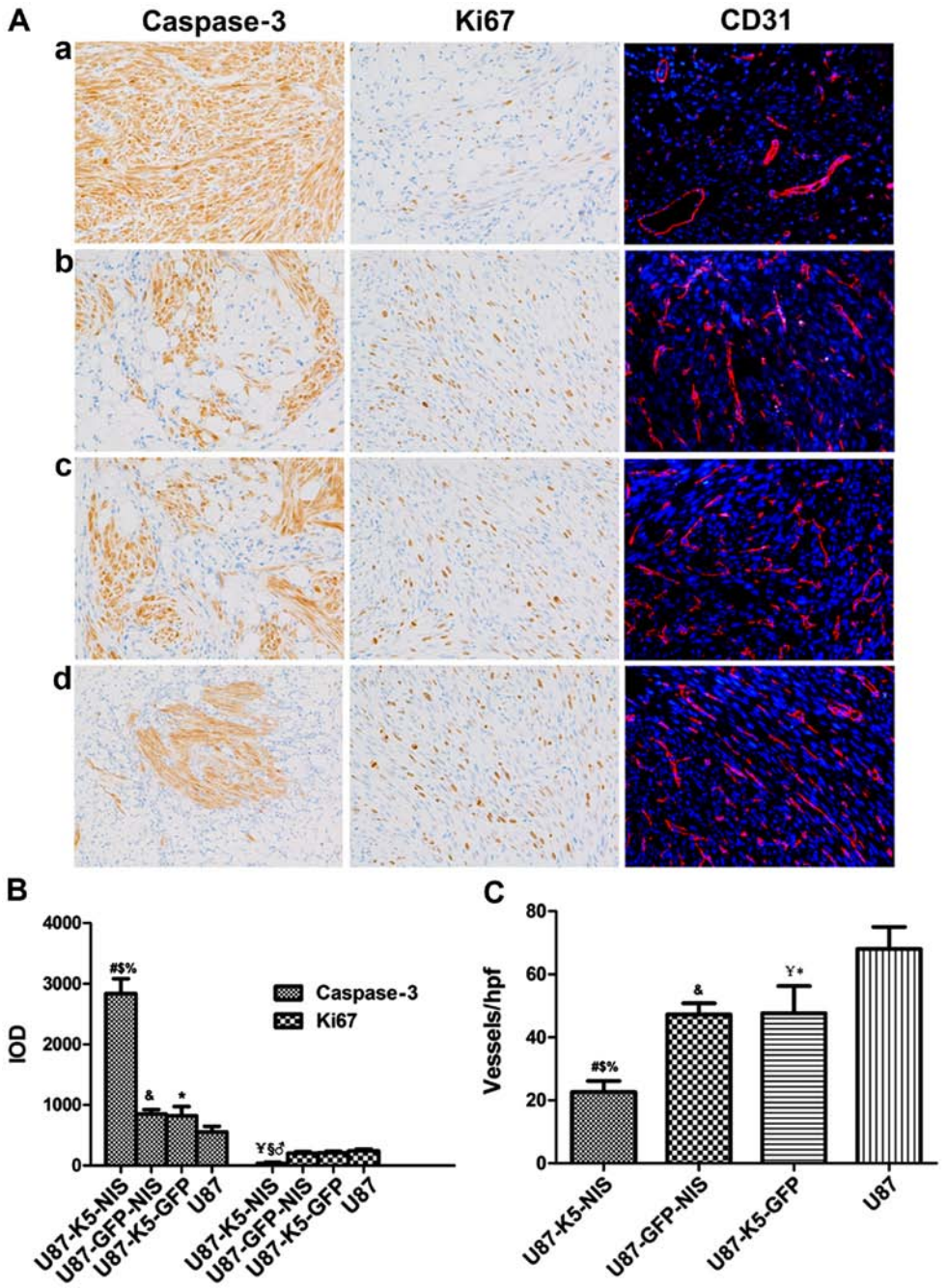

Figure 7. Immunohistochemical and immunofluorescence analysis. (A) Expression of caspase-3, Ki-67 and CD31 in U87-K5-NIS, U87-K5-GFP, U87-GFP-NIS and U87 xenograft tumors treated with ^{131}I (magnification, x200; a-d, U87-K5-NIS, U87-K5-GFP, U87-GFP-NIS and U87 xenograft tumor tissues). (B) Immunohistochemical analysis of protein caspase-3 and Ki67 ($^{\#}$p<0.001 vs. U87-GFP-NIS; $^{\$}$p<0.001 vs. U87-K5-GFP; $^{\%}$p<0.001 vs. U87; $^{\&}$p<0.01 vs. U87; *p<0.01 vs. U87; $^{¥}$p<0.05 vs. U87-GFP-NIS; $^{\$}$p<0.05 vs. U87-K5-GFP; and $^{♂}$p<0.05 vs. U87 group). (C) The capillary density of vessels positive for CD31 ($^{\#}$p<0.01 vs. U87-GFP-NIS group; $^{\$}$p<0.01 vs. U87-K5-GFP group; $^{\%}$p<0.001 vs. U87 group; $^{\&}$p<0.05 vs. U87 group; $^{¥}$p<0.05 vs. U87-GFP-NIS group; *p<0.05 vs. U87 group. Density was defined as the number of CD31^{+} endothelial cells per high-power field (hpf) (x200). Data are present as means ± SD.

combination therapy increased tumor cell apoptosis, inhibited tumor cell proliferation and significantly reduced capillary density in the U87 glioma tissues.

Gliomas are tumors that arise from glial or glial progenitor cells in the central nervous system. The median survival time of patients with malignant glioma is <3 years (19) and is even shorter in the event of recurrence, usually 3-6 months (20). A combination of chemotherapy or stereotactic radiosurgery with repeated surgery was previously found to improve the survival of patients with recurrent GBM compared to surgery alone, although no patient in the study survived beyond 44 weeks after treatment (21). However, the use of radiotherapy is limited in recurrent tumors due to the associated irreversible brain tissue damage and radiation-induced necrosis of the normal brain (22) highlighting the need for new therapeutic strategies. Given the following advantages, ^{131}I therapy, which is mediated by the *NIS* gene, is used for treating thyroid cancer in the clinic. ^{131}I expends 971 KeV decay energy, with γ decay following rapidly after β decay. The electrons have only 0.6-2 mm tissue penetration (23) causing a low degree

of injury to the healthy tissues around the tumor. This indicates that ^{131}I, mediated by the ectopic *NIS* gene, may have significant potential as an effective low-toxic treatment for glioma. Previous studies have demonstrated that *NIS* can be transferred into a variety of tumors, including nasopharyngeal carcinoma (17) breast cancer (24), glioma (6) and prostate carcinoma (25) and is capable of ^{131}I uptake and has different inhibitory actions on tumor growth. However, intracellular iodine is rapidly released, resulting in limited radioiodide retention time within cells; therefore, ^{131}I therapeutic efficacy is limited. To resolve this issue, we used a radio-inducible Egr1 promoter to promote NIS expression, creating an ^{131}I radiation positive feedback effect to increase NIS protein expression levels, increasing the ^{131}I retention time and the amount in the cells. For neovascularized tumors, neovasculature-targeting therapy is a promising prospect that is aimed at destroying the blood vessels, thus depriving tumor cells of oxygen and nutrients. K5 displays its potent anti-angiogenic effect by inducing EC apoptosis (13,14). Moreover, inhibition of angiogenesis was observed when colorectal carcinoma cells stably expressing K5 were propagated subcutaneously in athymic nude mice (26).

We successfully constructed the lentiviral vectors pLVX-CMV-K5-Egr1-NIS, pLVX-CMV-K5-Egr1-GFP and pLVX-CMV-GFP-Egr1-NIS, constructing the stable cell lines U87-K5-NIS, U87-K5-GFP and U87-GFP-NIS following lentiviral transduction and puromycin selection. K5 was expressed in U87-K5-NIS and U87-K5-GFP cells and their supernatant but not in U87-GFP-NIS and U87 cells or their supernatant; NIS was expressed in U87-K5-NIS and U87-GFP-NIS cells but not in U87-K5-GFP and U87 cells. There was higher NIS expression following a 24-h ^{131}I irradiation in U87-K5-NIS and U87-GFP-NIS cells. Guo *et al* reported more NIS staining by immunofluorescence testing *in vitro* following ^{131}I (7.4 MBq/ml) irradiation in Bac-Egr1-hNIS-transduced glioma cells (10). *In vivo* microSPECT/CT imaging showed more significant radioactive uptake (0.3243±0.0333 μCi/mm^3) in U87-K5-NIS tumors two days after irradiation with 18.5 MBq ^{125}I as compared with U87-K5-NIS tumors without ^{125}I irradiation (0.1240±0.0201 μCi/mm^3) ($P<0.001$). These studies showed that the Egr1 promoter may be useful for increasing NIS protein expression and for increasing NIS radioiodide accumulation.

The *in vitro* clonogenic assays showed that the medium containing K5 secreted by U87-K5-NIS and U87-K5-GFP cells had a significant cytotoxic effect on HUVECs as compared to that of U87-GFP-NIS and U87 cells ($P<0.05$). At 25 days after ^{131}I administration, immunofluorescence showed a lower density of CD31$^+$ capillaries in the U87-K5-NIS group as compared with the other three groups. Lower-density CD31$^+$ capillaries were also observed in the U87-K5-GFP group compared with the U87-GFP-NIS ($P<0.05$) and U87 ($P<0.05$) groups. Ki-67 and caspase-3 immunohistochemical analysis revealed significantly fewer proliferating cells and increased apoptosis following ^{131}I treatment in U87-K5-NIS tumors as compared to the other three groups. K5 combined with ^{131}I significantly inhibited U87-K5-NIS tumor growth. These results showed that NIS-mediated ^{131}I irradiation therapy combined with *K5* gene therapy was superior to single-gene therapy alone. Not only did NIS-mediated ^{131}I irradiation increase EC sensitivity to K5-induced apoptosis, K5 increased the ^{131}I-mediated glioma cell apoptosis.

There are various limitations to the present study. First, although lentiviral vectors can infect both non-dividing and dividing cells (27), induce long-term expression of transgenes and lack antigenicity (28,29), genetic modification with lentiviral vectors in general and stable integration of the therapeutic gene into the host cell genome raise concerns regarding personal or environmental safety (30). Second, we constructed stable cell lines to study the efficacy of the combined gene therapy, which did not conform to clinical treatment. In the clinic, viruses are injected directly or i.v. into tumors. Therefore, tumor-specific promoters *in vivo* are advantageous due to their lower sensitivity to promoter inactivation and lower risk of activating the host cell defense machinery (31). Previously, we showed that NIS expression under the human telomerase reverse transcriptase (hTERT) promoter was similar to that under the CMV promoter and that the hTERT promoter may have not only specificity but also relatively strong transcriptional activity for targeted gene expression (5).

In conclusion, the Egr1 promoter induced an ^{131}I radiation positive feedback effect mediated by NIS. K5 increased ^{131}I-mediated glioma cell apoptosis; ^{131}I irradiation also increased EC sensitivity to K5-induced apoptosis. This combined gene therapy had a synergistic effect on therapeutic antitumor efficacy in glioma, inhibiting U87 cell proliferation, arresting angiogenesis and retarding U87 tumor growth more effectively than single-gene therapy alone.

Acknowledgements

The present study was supported by grants from the National Natural Science Foundation of China (nos. 81071181, 81271610 and 81471686), the Shanghai Outstanding Academic Leaders Project (11XD1403700), and the Discipline Leaders Climbing Project of Ruijin Hospital and Shanghai Health Bureau Youth Foundation (2010Y021). We are also indebted to the staff of the Department of Nuclear Medicine, Fudan University Shanghai Cancer Center for their technological support with micro-SPECT/CT imaging.

References

1. Chung JK: Sodium iodide symporter: Its role in nuclear medicine. J Nucl Med 43: 1188-1200, 2002.
2. Verburg FA, de Keizer B, Lips CJ, Zelissen PM and de Klerk JM: Prognostic significance of successful ablation with radioiodine of differentiated thyroid cancer patients. Eur J Endocrinol 152: 33-37, 2005.
3. Hackshaw A, Harmer C, Mallick U, Haq M and Franklyn JA: ^{131}I activity for remnant ablation in patients with differentiated thyroid cancer: A systematic review. J Clin Endocrinol Metab 92: 28-38, 2007.
4. Chung JK, Youn HW, Kang JH, Lee HY and Kang KW: Sodium iodide symporter and the radioiodine treatment of thyroid carcinoma. Nucl Med Mol Imaging 44: 4-14, 2010.
5. Zhang M, Guo R, Shi S, Miao Y, Zhang Y and Li B: Baculovirus vector-mediated transfer of sodium iodide symporter and plasminogen kringle 5 genes for tumor radioiodide therapy. PLoS One 9: e92326, 2014.
6. Guo R, Zhang M, Xi Y, Ma Y, Liang S, Shi S, Miao Y and Li B: Theranostic studies of human sodium iodide symporter imaging and therapy using ^{188}Re: A human glioma study in mice. PLoS One 9: e102011, 2014.

7. Kim YH, Youn H, Na J, Hong KJ, Kang KW, Lee DS and Chung JK: Codon-optimized human sodium iodide symporter (opt-hNIS) as a sensitive reporter and efficient therapeutic gene. Theranostics 5: 86-96, 2015.
8. Vadysirisack DD, Shen DH and Jhiang SM: Correlation of Na^+/I^- symporter expression and activity: Implications of Na^+/I^- symporter as an imaging reporter gene. J Nucl Med 47: 182-190, 2006.
9. Wagner M, Schmelz K, Dörken B and Tamm I: Transcriptional regulation of human *survivin* by early growth response (Egr)-1 transcription factor. Int J Cancer 122: 1278-1287, 2008.
10. Guo R, Tian L, Han B, Xu H, Zhang M and Li B: Feasibility of a novel positive feedback effect of ^{131}I-promoted Bac-Egr1-hNIS expression in malignant glioma via baculovirus. Nucl Med Biol 38: 599-604, 2011.
11. Gorski DH, Beckett MA, Jaskowiak NT, Calvin DP, Mauceri HJ, Salloum RM, Seetharam S, Koons A, Hari DM, Kufe DW, *et al*: Blockage of the vascular endothelial growth factor stress response increases the antitumor effects of ionizing radiation. Cancer Res 59: 3374-3378, 1999.
12. Zhu X, Palmer MR, Makrigiorgos GM and Kassis AI: Solid-tumor radionuclide therapy dosimetry: New paradigms in view of tumor microenvironment and angiogenesis. Med Phys 37: 2974-2984, 2010.
13. Davidson DJ, Haskell C, Majest S, Kherzai A, Egan DA, Walter KA, Schneider A, Gubbins EF, Solomon L, Chen Z, *et al*: Kringle 5 of human plasminogen induces apoptosis of endothelial and tumor cells through surface-expressed glucose-regulated protein 78. Cancer Res 65: 4663-4672, 2005.
14. Lu H, Dhanabal M, Volk R, Waterman MJ, Ramchandran R, Knebelmann B, Segal M and Sukhatme VP: Kringle 5 causes cell cycle arrest and apoptosis of endothelial cells. Biochem Biophys Res Commun 258: 668-673, 1999.
15. Cao Y, Chen A, An SS, Ji RW, Davidson D and Llinás M: Kringle 5 of plasminogen is a novel inhibitor of endothelial cell growth. J Biol Chem 272: 22924-22928, 1997.
16. Blezinger P, Wang J, Gondo M, Quezada A, Mehrens D, French M, Singhal A, Sullivan S, Rolland A, Ralston R, *et al*: Systemic inhibition of tumor growth and tumor metastases by intramuscular administration of the endostatin gene. Nat Biotechnol 17: 343-348, 1999.
17. Shi S, Zhang M, Guo R, Miao Y, Hu J, Xi Y and Li B: In vivo molecular imaging and radionuclide (^{131}I) therapy of human nasopharyngeal carcinoma cells transfected with a lentivirus expressing sodium iodide symporter. PLoS One 10: e0116531, 2015.
18. Sides MD, Sosulski ml, Luo F, Lin Z, Flemington EK and Lasky JA: Co-treatment with arsenic trioxide and ganciclovir reduces tumor volume in a murine xenograft model of nasopharyngeal carcinoma. Virol J 10: 152, 2013.
19. Chamberlain MC: Emerging clinical principles on the use of bevacizumab for the treatment of malignant gliomas. Cancer 116: 3988-3999, 2010.
20. Niyazi M, Siefert A, Schwarz SB, Ganswindt U, Kreth FW, Tonn JC and Belka C: Therapeutic options for recurrent malignant glioma. Radiother Oncol 98: 1-14, 2011.
21. Mandl ES, Dirven CM, Buis DR, Postma TJ and Vandertop WP: Repeated surgery for glioblastoma multiforme: Only in combination with other salvage therapy. Surg Neurol 69: 506-509, 2008.
22. Mayer R and Sminia P: Reirradiation tolerance of the human brain. Int J Radiat Oncol Biol Phys 70: 1350-1360, 2008.
23. Skugor M: The Cleveland Clinic Guide to Thyroid Disorders. Kaplan Publisher, New York, 2006.
24. Dwyer RM, Bergert ER, O'connor MK, Gendler SJ and Morris JC: In vivo radioiodide imaging and treatment of breast cancer xenografts after MUC1-driven expression of the sodium iodide symporter. Clin Cancer Res 11: 1483-1489, 2005.
25. Dwyer RM, Schatz SM, Bergert ER, Myers RM, Harvey ME, Classic KL, Blanco MC, Frisk CS, Marler RJ and Davis BJ: A preclinical large animal model of adenovirus-mediated expression of the sodium-iodide symporter for radioiodide imaging and therapy of locally recurrent prostate cancer. Mol Ther 12: 835-841, 2005.
26. Liu XY, Qiu SB, Zou WG, Pei ZF, Gu JF, Luo CX, Ruan HM, Chen Y, Qi YP and Qian C: Effective gene-virotherapy for complete eradication of tumor mediated by the combination of hTRAIL (TNFSF10) and plasminogen k5. Mol Ther 11: 531-541, 2005.
27. Naldini L, Blömer U, Gallay P, Ory D, Mulligan R, Gage FH, Verma IM and Trono D: In vivo gene delivery and stable transduction of nondividing cells by a lentiviral vector. Science 272: 263-267, 1996.
28. Sakuma T, Barry MA and Ikeda Y: Lentiviral vectors: Basic to translational. Biochem J 443: 603-618, 2012.
29. Charrier S, Stockholm D, Seye K, Opolon P, Taveau M, Gross DA, Bucher-Laurent S, Delenda C, Vainchenker W, Danos O, *et al*: A lentiviral vector encoding the human Wiskott-Aldrich syndrome protein corrects immune and cytoskeletal defects in WASP knockout mice. Gene Ther 12: 597-606, 2005.
30. Rothe M, Modlich U and Schambach A: Biosafety challenges for use of lentiviral vectors in gene therapy. Curr Gene Ther 13: 453-468, 2013.
31. Liu BH, Wang X, Ma YX and Wang S: CMV enhancer/human PDGF-beta promoter for neuron-specific transgene expression. Gene Ther 11: 52-60, 2004.